DESIGN AND CONTROL OF POWER CONDITIONING UNIT FOR FCHV USING MFOA

P.V.Gokila
Department of Electrical and Electronics Engineering
J.K.K.Nataraja College of Engineering and Technology,Kumarapalayam, TamilNadu,India

Abstract- **The output of the renewable energy sources are low voltage and high current for the designed power rating. Since the output is of low voltage it cannot meet the load demands that require high voltages. Therefore to satisfy the necessity of high voltage loads, power converter (DC-DC) are used to maximize the voltage. The DC output voltage from renewable energy sources is given as input to DC-DC converters and also the output from the converter is used to drive the load. The voltage regulator is an electronic circuit that is specifically designed to supply a very stable DC output voltage even if large variations occur within the input. KY boost converter is one of the recently invented DC-DC converter topology with reduced output voltage ripple. It is suitable for device to operate below low ripple condition. The most drawback of this converter is that the voltage boosting is low for designed parameters. To obtain the required boosted voltage and to reduce the output voltage ripple, Optimization Algorithm is used. The Fruit Fly Optimization technique is the convergence characteristics is higher and the output ripple is higher, when compared with the proposed work The Modified Fruit fly Optimization Algorithm (MFOA) technique is compared with the existing Fruit Fly Optimization Algorithm (FOA) technique in the feedback loop. Simulation results are obtained using MATLAB and hardware results validate the proposed methodology.**

Keywords- fruit fly optimization,modified fruitfly optimization,converter.

I. INTRODUCTION

The problems related to the supply of oil, pollution and the greenhouse effect justify the need to develop new technologies for the transportation as a replacement for the actual technology based on internal combustion engines. Fuel cells promise that the best pace that they operate more efficiently and with fewer emissions. A hybrid propulsion system, which combines two sources:

• Fuel cell is the main source. It is the electrochemical device that converts the chemical energy of a reaction directly into electrical energy. The stack has a slow dynamics done allowing him to answer to an increase or a rapid decrease in the output power as well as the recovery of the energy.

• The super-capacitor is the source of storage; it has significant capacity but a low voltage. It can restore the energy more quickly as a battery.

It presents the following advantages:

- Provide additional power rapid during peak periods such as the acceleration
- Enable the recovery of the braking energy by the recovery and store it in the super-capacitor, thus increasing the overall efficiency of the vehicle.

The adaptation of the levels of the voltage between the two sources and the load in the vehicle requires the converter (KY boost converter) to maintain constant the voltage of the DC bus allowing imposing the power or the current required by the load.The other converter is an inverter, it is used to adapt the voltage levels between the DC link and the PMSM (Permanent Magnet Synchronous Motor). In the stationary state, the fuel cell stack must produce the energy required to move the electric vehicle. The fuel cell will become the primary energy source for the next generation of hybrid electric vehicles.

This paper proposes KY boost converter working in minimum voltage ripple used in HEV between battery and inveter feed permanent synchronous motor (PMSM). The proposed technology has benefits such as to minimum size of passive component, reducing input current ripple, make the system more reliable in high power application, increasing the converter efficiency, decreasing the voltage and current ratings of power electronics devices these above metioned advantages of proposed converter makes it more reliable in high power hybrid electrical vehicle applications

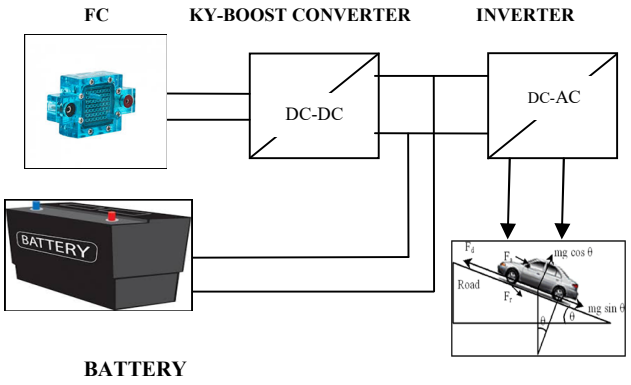

Fig 1 Block diagram of FCHV

II. DYNAMICS OF THE VEHICLE

Based on principles of vehicle mechanic, the various forces and the moving vehicle are presented in Fig. 2.Three main resistances forces $\mathbf{F_A}$, $\mathbf{F_X}$ and $\mathbf{F_R}$ called respectively aerodynemic force, rolling resistance force and gravity force. The tensile force FX propels the vehicle forward. The propulsion system (the permanent magnet synchronous motor) must provide the necessary force to the vehicle traction at the wheels. This force must firstly provide the necessary effort to speed and partly overcome the resistant force to the coil, the aerodynamic force and road inclination[15].

• Rolling resistance force: The rolling resistance force acts on the level of tires and is opposed to the free movement of the vehicle. It is caused by the deformation of the tires on the road way which generates a rolling friction. It depends on the vehicle mass M (kg), the acceleration of gravity (m.s-2) and the rolling resistance coefficient C_R.

$$F_{\_R}=MgC_R \quad (1)$$

The gravity force affects immediately the vehicle on the slope. It retains it in rise and pushes it in descent. It depends on the inclination of the slope and the vehicle mass M.

$$F_{\_G}=Mgsin(\theta) \quad (2)$$

• Aerodynamic Force: This is the air resistance force. It varies depending on the vehicle speed and depends on non-linear phenomena within the fluid mechanics. It is proportional to the air density ñ (Kg/m3), to the front section S_f (m2) of the vehicle, the drag coefficient C_x of the air and vehicle speed V (ms-1).

$$F_A = \frac{\rho C_x S_f V^2}{2} \quad (3)$$

• Traction force: It indicates the force which is exerted on the periphery of the driving wheels in contact with the ground to create or maintain the movement of the vehicle. The magnitude force depends on the motor torque, gear transmission and the radiusof the wheels.

$$F_x(t) = M\frac{dV(t)}{dt} + Mgsin(\theta) + \frac{\rho C_x S_f V^2}{2} + MgC_R \quad (4)$$

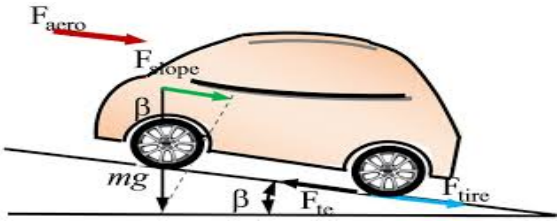

Fig.2- The forces acting on a vehicle moving on slope road

Table 1-Parameters of the electric vehicle model

Vehicle parameters	Symbol	Values	Unit
Drag coefficient	C_R	0.062	
Aerodynamic frontal area	A	0.0016	m^2

Mass	M	104	Kg
Rolling coefficient of tire	μ_{rr}	0.0025	
Traction wheel diameter	R	0.2425	M

III.PMSM MODEL

The PMSM control is equivalent to that the dc motor by a decoupling control known as field oriented control or vector control. The vector control separates the torque component of current and flux channels in the motor through its stator excitation. The vector control of PM synchronous motor is derived from it dynamic model. Considering the currents as inputs, the three currents are:

$$i_a = I_s \sin(\omega_r t + \alpha)$$
$$i_b = I_s \sin(\omega_r t + \alpha - \frac{2\pi}{3})$$
$$i_c = I_s \sin(\omega_r t + \alpha + \frac{2\pi}{3}) \quad (5)$$

where α is the angle between the rotor field and stator current phasor , is the electrical rotor speed. The previous currents obtained are stator currents that must be transformed to the rotor reference frame with the rotor speed , using Park's transformation. The q and d axis currents are constants in the rotor reference frame since α is a constant for given load torque. As these contants, they are similar to the armature and field currents in the separately exicted dc machine. The q axis current is distinctly equivalent to the armature current of the dc machine; the d axis current is field current , but not in its entirely. It is only a partial field current; the other part is contributed by the equivalent current source representing the permanent magnet field. For this reason the q axis current is called the torque producing component of the stator current and the d axis current is called the flux producing component of the stator current. and in terms of as follows:

$$\begin{pmatrix} i_q \\ i_d \end{pmatrix} = I_s \begin{pmatrix} sin\alpha \\ cos\alpha \end{pmatrix} \quad (6)$$

In the constant torque equation, if =0 and by δ=90̊ then the electric torque equation becomes

$$T_e = \left(\frac{3}{2}\right)\left(\frac{p}{2}\right)\lambda_{af} I_q \quad (7)$$

In the flux weakening region where > angle α is controlled by proper control of and for the same value of the stator current. Since is reduced the output torque is also reduced. The angle α can be obtained as:

$$\alpha = \tan^{-1}\left(\frac{i_q}{i_d}\right) \quad (8)$$

The current is related to and by:

$$I_s = \sqrt{i_q^2 + i_d^2} \quad (9)$$

Using α and rotor position the controller will generate the reference currents; then the current controller makes uses of the reference signals to control th inverter for the desired output currents. The load torque is adjusted to the maximum available torque for the reference speed:

$$T_L = T_{e(rated)}\left(\frac{\omega_{rated}}{\omega_r}\right) \quad (10)$$

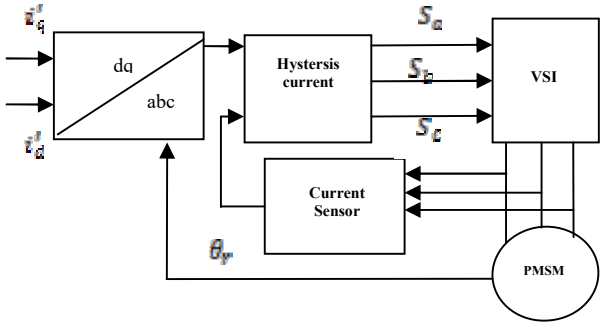

Fig 4-PMSM model

For PM motor drive system with a full speed range he system will consist of a motor, an inverter, a controller(constant torque and flux weakening operation, generation of reference currents and PI controller) as shown in figure 4.

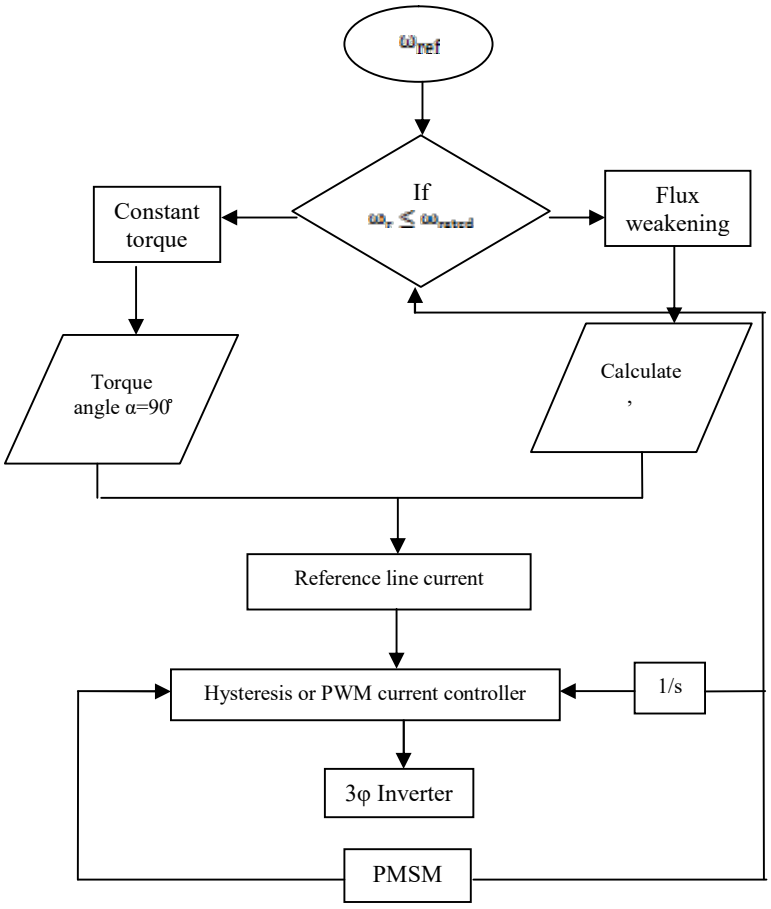

Fig 3- Flow chart of PMSM model

The operation of the controller must be done according to the speed range. For operation up to rated speed it will operate in constant torque region and for speeds above rated it will operate in the flux-weakening region. In this region, the d-axis flux and the developed torque are reduced. The process can be understood with the flow diagram in figure.3.

IV FUEL CELL MODEL

A fuel cell is an energy conversion system that converts chemical energy into electrical energy without any thermal or mechanical process. The operating principle of a fuel cell is described by a chemical reaction that reacted hydrogen and oxygen to produce electricity, heat, and water, according to the chemical reaction given by equation 13

$$H_2 + \frac{1}{2}O_2 \longrightarrow H_2O + \text{heat} + \text{electrical energy} \quad (11)$$

There are many fuel cell models; each model has its own specificities and benefits, according to the phenomena studied. The chosen model should be simple and accurate.

Indeed, this work presents an electrochemical model which can be used to predict the fuel cell behavior in static and dynamic conditions

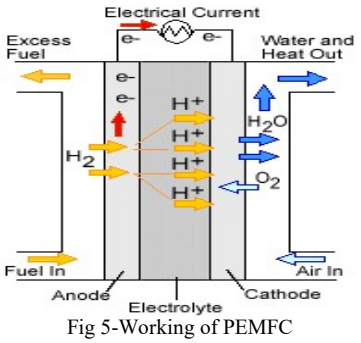

Fig 5-Working of PEMFC

The fuel cell voltage depends on the partial pressures of hydrogen and oxygen, the chemical reaction temperature of the membrane hydration and the output current. It is defined by the following equation

$$V_{FC} = V_{nett} - V_{act} - V_{ohm} - V_{cons} \quad (12)$$

V KY BOOST CONVERTER

Figure 6 shows the proposed positive –voltage KY boost converter composed of the KY converter combined with the traditional boost converter, which is described as follows. The KY converter is consist of the switches S1 and S2 , the diode Db, the energy –transferring capacitor Cb , the output capacitor C0. The input of the KY converter is retrieved by the buffer capacitor Cm. on the other hand, the traditional boost converter consists of the switches S1 and S2, the input inductor Li. The output of the conventional boost converter is replaced by the buffer capacitor Cm. The buffer capacitor Cm is a buffer between the KY boost converter and the traditional boost converter. The output load is represented by the represented by the load resistor RL.

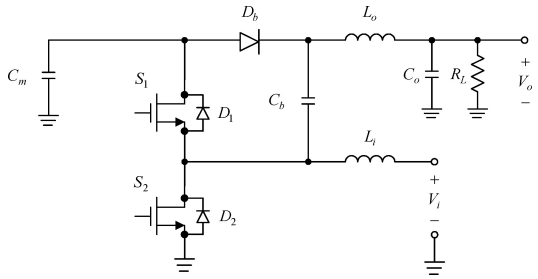

Fig 6-KY boost converter

- 5.1 Mode1 operation of KY boost converter.

In figure 7. S1 is turned off and S2 is turned on. In this case, the negative terminal of C b is pulled to the ground and hence Db is forward biased and turned on. During this mode, Cm is discharged whereas Cb is charged. Therefore, the voltage across Li is Vi, thereby causing Li to be magnetized, whereas the voltage across L0 is V0 subtracted from VCm, thereby causing L0 to be demagnetized. Also, the current flowing through C0 is equal to iL0 minus the current flowing through RL. And hence, the corresponding differential equations are.

$$\begin{cases} V_{L_i} = L_i \frac{\partial i_{L_i}}{\partial t} \\ L_0 \frac{\partial i_{L_0}}{\partial t} = V_{C_m} + V_0 \\ C_m \frac{\partial V_{C_m}}{\partial x} = -i_{C_b} - i_{L_0} \\ C_0 \frac{\partial V_0}{\partial x} = i_{L_0} - \frac{V_0}{R} \end{cases} \quad (13)$$

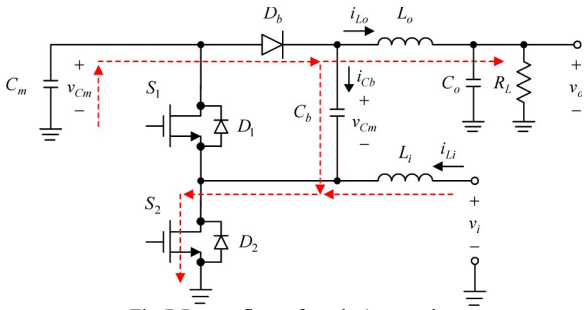

Fig 7-Power flow of mode 1 operation

- Mode 2 operation KY boost converter

In the figure, 8 S1 is turned on and S2 is turned off. In this case, S1 is in the on-state and hence Db is reverse biased and turned off. During this mode, Cm is charged whereas Cb is discharged. Therefore, the voltage across Li is V_{Cm} subtracted from Vi, thereby causing Li to be demagnetized, whereas the voltage across L0 is subtracted from the sum of and , thereby causing L0 to be magnetized. Also , the current flowing through is equal to minus the current flowing through . And hence, the corresponding differential equations are

$$\begin{cases} L_i \frac{\partial i_{L_0}}{\partial x} = V_i - V_{C_m} \\ L_0 \frac{\partial i_{L_0}}{\partial x} = 2V_{C_m} - V_0 \\ C_m \frac{\partial v_{C_m}}{\partial x} = i_{L_i} - i_{L_0} \\ C_0 \frac{\partial V_0}{\partial x} = i_{L_0} - \frac{V_0}{R} \end{cases} \quad (14)$$

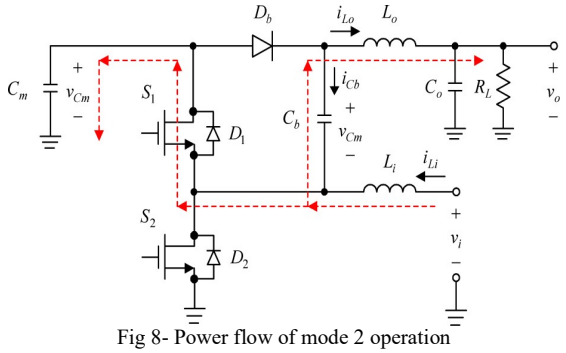

Fig 8- Power flow of mode 2 operation

The average equations which are obtained from the equation () to equation (),

$$L_i \frac{\partial iL_i}{\partial t} = (V_i) - (1-d)(V_{C_m})$$

$$C_0 \frac{\partial i_{L_0}}{\partial t} = (iL_0)$$

$$L_0 \frac{\partial i_{L_0}}{\partial t} = (2-d)(V_{C_m}) - (V_0)$$

$$C_m \frac{\partial V_{C_m}}{\partial t} = (-i_{L_0}) + (1-d)(i_{L_i}) - d(i_{C_b})$$

$$\frac{C_b}{C_m} = \frac{\left(\left(\frac{1-d}{d}\right)(i_{L_0})\right)}{\left(-\left(\frac{1-d}{d}\right)(i_{L_0}) + i_{L_i}(1-d) - (i_{L_0})\right)} \quad (15)$$

According to the small-ripple approximation and the voltage-second balance, the voltage ratio can be obtained to be

$$\frac{V_0}{V_i} = \frac{2-d}{1-d} \quad (16)$$

Where,

d=duty cycle, is the output voltage in Volts and is the input voltage in Volts.

Table 2-Specifications of KY boost converter

Parameter	Symbol	Value	Unit
Input voltage	V_i	12	V
Rated output voltage	V_o	36	V
Rated load current	I_o	10.36	A
Output inductance	L_o	3.623	mH
Buffer capacitance	C_m	31.24	mF
Energy transferring capacitor	C_b	62.2	mF
Output capacitance	C_o	470	µF
Switching Frequency	f_s	195	kHz
Load	Separately excited motor	0.5	Hp
Input inductance	L_i	0.402	mH

VI MODELING OF MFOA

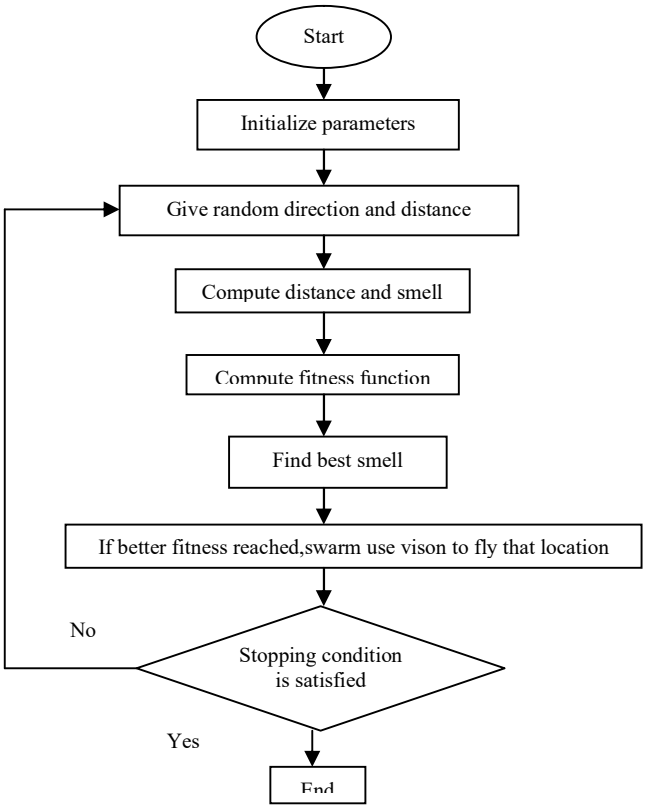

Fig 9-Flow chart of MFOA

Modified fruit fly optimization algorithm is a new method for deducing global optimization based on the foraging behavior of the fruit fly. The sensory perception of the fruit fly is better than that of other species, especially the sense of smell and vision. The olfactory organ of a fruit fly can gather various smells from the air, and even a food source 40 km away. Then, after it gets close to the food location (optimal value), it can also use its sensitive vision to find food and the company's flocking location, and fly towards that direction too.
Generally, the procedures of MFOA for an optimization problem solving including:

a. The random initial position of a fruit fly swarm , Init X_axis, Init Y_axis , Init Z_axis.
b. Random direction and distance of searching for food using the sense of smell of a fruit fly individual.
    i. X_i=X_axis+ Random Value
    ii. Y_i =Y_axis+ Random Value
    iii. Z_i =Z_axis+ Random Value
c. As the location of food cannot be known, the distance (Dist) to the origin is estimated before the decision value of smell concentration (S) is calculated; this value is reciprocal of distance.
    i. $Dist_i = \sqrt{X_i^2 + Y_i^2} + Z_i^2$
    ii. $S_i = \frac{1}{Dist_i} + B$
    iii. B= $Dist_i$*(0.5-rand())
d. The smell concentration decision value (S) is substituted in the smell concentration decision function (also known as the Fitness function) to work out the smell concentration (S_i) in the position of the fruit fly individual.
    i. Smell=Function(S_i)
e. Determine the fruit fly with maximum smell concentration among the fruit fly swarm (seek for the maximum value).

[bestSmellbestIndex]=max(Smell)

a. Retain the best smell concentrations value and x,y coordinates, here the fruit fly swarm flies toward the position by vision.
    i. Smellbest =bestSmell
    ii. X_axis=X(bestIndex)
    iii. Y_axis=Y(bestIndex)
    iv. Z_axis=Z(bestIndex)
b. Enter into iterative optimization, repeat execution steps 2-5, and judge whether the smell concentration is better than the previous iterative smell concentration, if yes, execute Step 6.

Figure 10 shows the overall FCHV powertrain in MATLAB/Simulink. Figure 11 shows the FCHV-Electrical subsystem in MATLAB/Simulink. Figure 12 shows the KY boost converter with MFOA in Matlab/Simulink.

Figure 13 shows the output waveform of FCHV using KY Boost converter with FOA. From this, it is observed that the output drive torque of FOA is 205.2 Nm the ripple range is 3.6 Nm in KY boost converter using FOA.

Figure 14 shows the output waveform of FCHV using KY Boost converter with MFOA. From this, it is observed that the output drive torque of MFOA is 202.25 Nm the ripple get reduced to 3.1 Nm by using KY Boost converter using MFOA.By comparing these two methods of the optimization, therefore KY boost converter of FCHV using MFOA is better than the KY boost converter of FCHV using FOA.

Figure 15 shows the convergence characteristics of FOA and MFOA. From this, it is observed that the convergence is reduced in the MFOA and it is better than the FOA characteristics.

Figure 16 shows the input and output waveform of the closed loop KY boost converter using Fruit Fly Optimization Algorithm (FOA) based controller. From this, it is observed that the input voltage and the output voltage of closed loop KY boost converter is 12V and 36.47V for 0.5 duty cycle.

Figure 17 shows the input and output waveform of the closed loop KY boost converter using Modified Fruit Fly Optimization Algorithm (MFOA) based controller. From this, it is observed that the input and output voltage of closed loop KY boost converter is 12V and 36V is for 0.5 duty cycle and the ripple range of closed loop system is very minimum which cannot be determined.

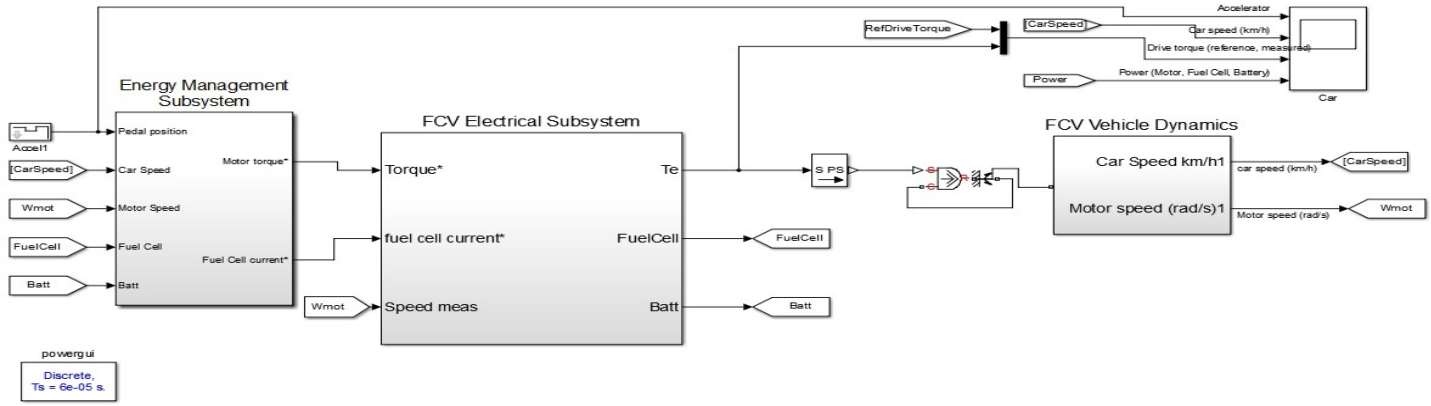

Fig 10-Overall FCHV powertrain

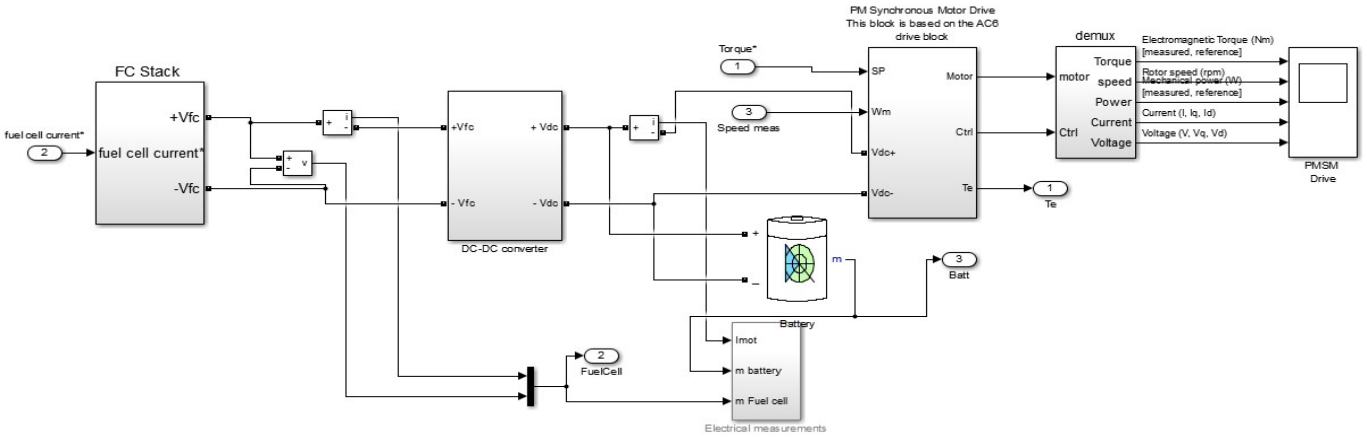

Fig 11-FCHV-Electrical subsystem

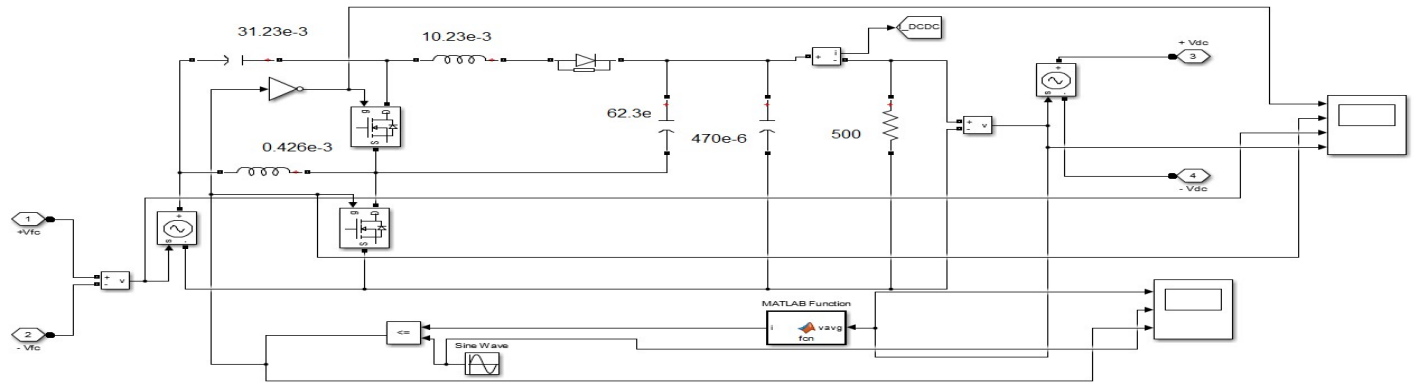

Fig 12-KY boost converter with MFOA

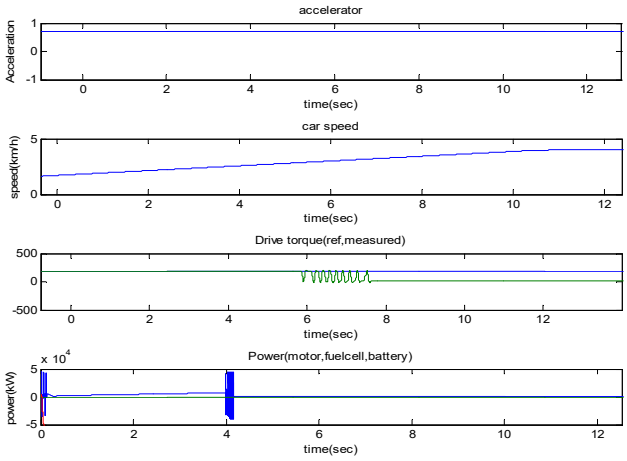

Fig 13-Output waveform of FCHV using KY boost converter with MFOA

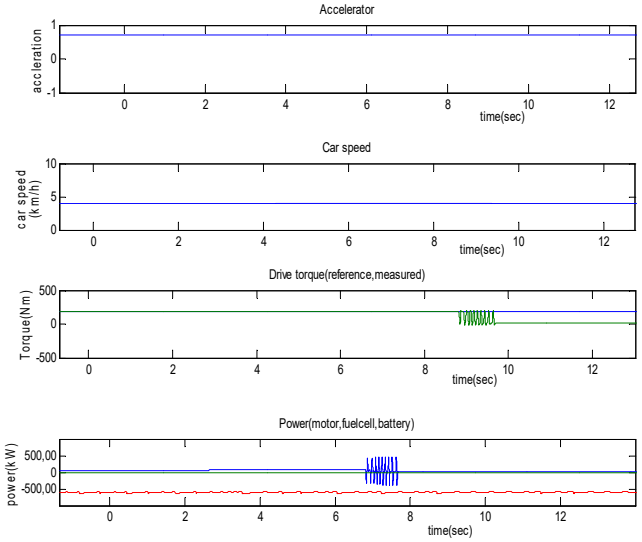

Fig 14-Output waveform of FCHV using KY boost converter with MFOA

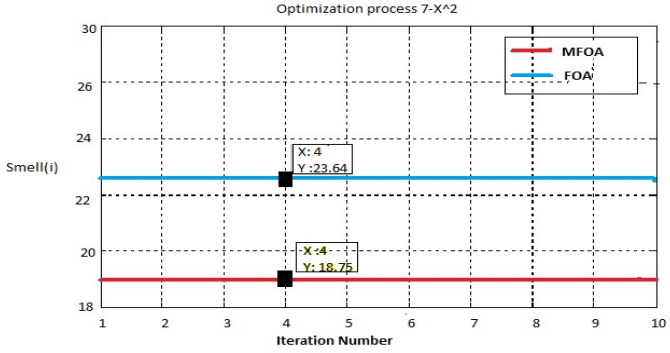

Fig 15 Convergence characteristics of FOA and MFOA

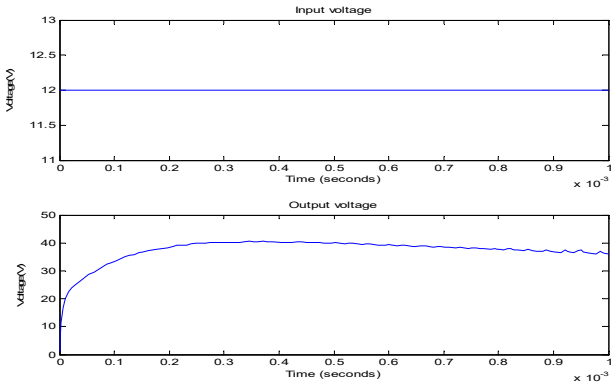

Fig 16-Output waveform of KY boost converter with FOA

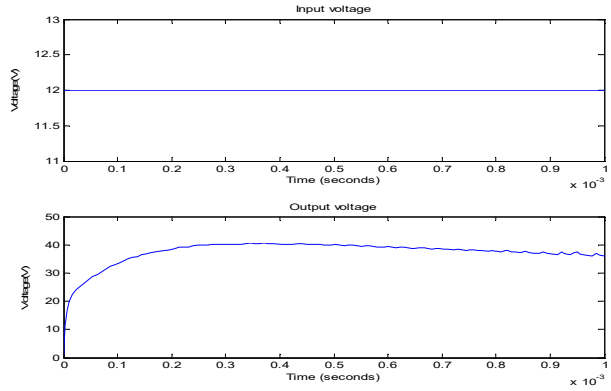

Fig 17-Output waveform of KY boost converter with MFOA

Table 3-Performance characteristics of FCHV using KY boost converter with FOA and MFOA

Parameters	**FCHV using KY Boost converter with FOA**	**FCHV using KY Boost converter with MFOA**
Output voltage	36.47V	36V
Ripple voltage	0.47V	the minimum amount of ripple which cannot be measured
Drive torque ripple	3.6 Nm	3.1 Nm

VII EXPERIMENTAL RESULTS

After testing the open loop and closed loop system of KY boost converter with simulation, real-time control is used to prove the effectiveness of the proposed converter. The control algorithm (MFOA) used in the Embedded C coding in the experimentation. An Atmega8controlleris used as a real-time controller in the experimentation. The KY boost converter has the sampling frequency of 20kHz for PWM generation in the hardware implementation. A photograph of the open and closed loop of converter experimental setup is shown in Fig and. As seen from the fig and fig, the output voltage ripple reduction is high in Modified Fruit Fly Optimization Algorithm(MFOA) based closed loop KY boost converter when compared to open loop system. As can be seen from this figure, the tracking responses are similar to the simulated results. And also from the fig, we observed that the expected output voltage (36V) was obtained even the input voltage vary and the maximum voltage transient due to step changes in the input voltages are about +/- 2V which is very less for MFOA based closed loop KY boost converter.

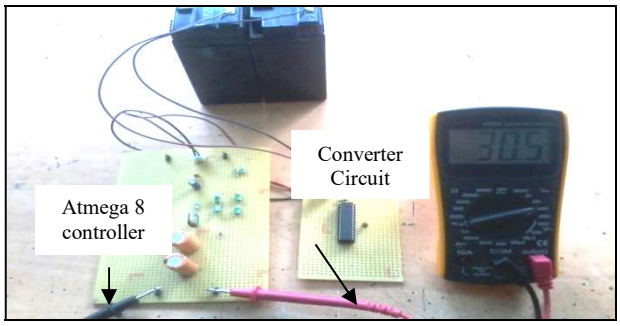

Fig 18 Hardware implementation of open loop KY boost converter

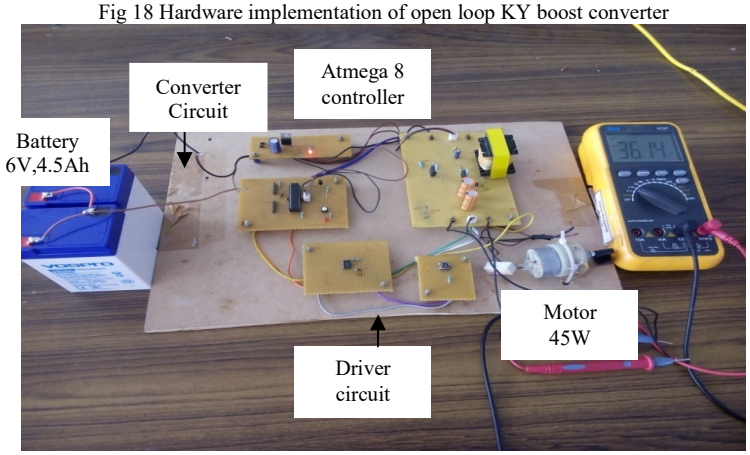

Fig 19-Hardware implementation of closed loop KY boost converter with MFOA

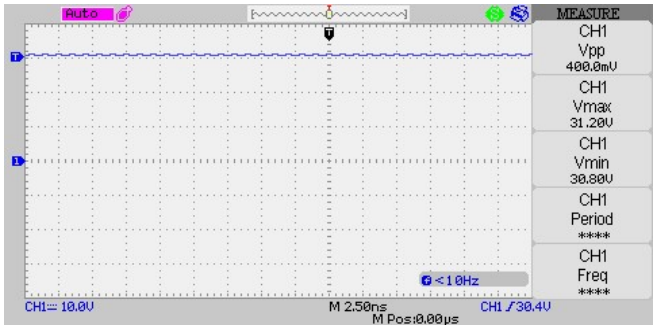

Fig 20-Output voltage waveform of KY boost converter in open loop condition

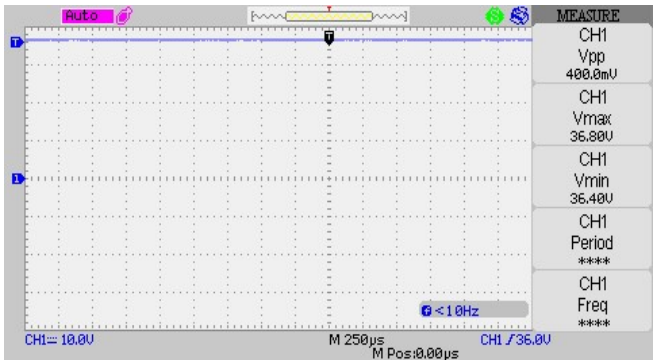

Fig 21 Output voltage waveform of KY boost converter in closed loop condition with MFOA

VIII CONCLUSION

The proposed work is simulated in MATLAB platform and the output waveform is evaluated. From the simulation, the fuel cell hybrid vehicle using KY boost converter with Fruit Fly Optimization (FOA) and Modified Fruit Fly Optimization (MFOA) is compared. The convergence characteristics are reduced and the output voltage ripple also reduced in a fuel cell hybrid vehicle using KY boost converter with Modified Fruit Fly Optimization. Then the hardware implementation is done for the proposed work and the result is validated for the simulation output.

REFERENCES

[1] Andari, Wahib, Samir Ghozzi, Hatem Allagui, and Abdelkader Mami. (2017)"Design, Modeling and Energy Management of a PEM Fuel Cell/Supercapacitor Hybrid Vehicle.", International Journal of Advanced Computer Science & Applications, Vol.1, No. 8,pp.273-278.

[2] Bernard, Jerome, Sebastien Delprat, Felix Buechi, and Thierry Marie Guerra (2006) “Global Optimisation in the power management of a Fuel Cell Hybrid Vehicle (FCHV)”, IEEE Conference on Vehicle Power and Propulsion Conference, VPPC”06. IEEE,Vol .pp.1-6

[3] Choubey, Nitin S (2014) “Fruit fly optimization algorithm for traveling salesperson problem”, International Journal of Computer Applications (0975–8887),pp.22-27.

[4] Fares, Dima, et al (2014) “Optimal power allocation for an FCHV based on linear programming and PID controller”, International Journal of Hydrogen Energy, No.39, Vol 36, pp.21724-21738.

[5] Gasbaoui, Brahim, Abdelfatah Nasri, Othmane Abdelkhalek, Jamel Ghouili, and Abdelkader Ghezouani. (2017)."Behavior PEM fuel cell for 4WD electric vehicle under different scenario consideration.", International Journal of Hydrogen Energy , Vol.420.pp535-543.

[6] Hwu, K. I., and Y. T. Yau (2010) “A KY boost converter” IEEE Transactions on Power Electronics, No.25, Vol.11,pp.2699-2703.

[7] Hwu, K. I., and Y. T. Yau(2009) “KY converter and its derivatives”, IEEE Transactions on Power Electronics, No.24, Vol.1,pp.128-137.

[8] Hwu, K. I., and W. Z. Jiang (2014) “Voltage gain enhancement for a step-up converter constructed by KY and buck-boost converters” IEEE Transactions on Industrial Electronics , No.61, Vol.4,pp.1758-1768.

[9] Iscan, Hazim, and Mesut Gunduz (2014) “Parameter analysis on fruit fly optimization algorithm”, Journal of Computer and Communications, No.2,Vol.04,pp.137.

[10] Kanaan, H. Y., S. Georges, I. Mougharbel, N. Mendalek, and T. Nicolas.(2009) "Modeling, Control and Simulation of a High-Current DC-DC Converter for Fuel Cell Applications.", In Proc. International Conference on Renewable Energy and Power Quality (ICREPQ'09), Valencia, Spain, Vol 1, No 7.

[11] Karthikumar, S, N. Mahendran, and S. Sriraman (2012) “Design of fuzzy logic controller for Output Voltage Ripple (OVR) reduction of KY boost converter”, International Conference on Emerging Trends in Electrical Engineering and Energy Management (ICETEEEM), IEEE,pp.181-185.

[12] Liu, Yi, Xuejie Wang, and Yanjun Li. (2012)"A modified fruit-fly optimization algorithm aided PID controller designing." In Intelligent Control and Automation (WCICA), 10th World Congress on 2012, pp. 233-238.

[13] Mokrani, Zahra, Djamila Rekioua, and Toufik Rekioua (2014) “Modeling, control and power management of hybrid photovoltaic fuel cells with battery bank supplying electric vehicle”, International Journal of Hydrogen Energy, No.39,Vol.27,pp.15178-15187.

[14] Montero, C., et al (2012) “Fuel cell and power control for a hybrid vehicle. Experimental results”, IECON 38th Annual Conference on IEEE Industrial Electronics Society, IEEE, pp. 4121-4126.